Inorg. Chem. **2008**, *47*, 9450−9458

High and Low Spin Mononuclear and Dinuclear Iron(II) Complexes of 4-Amino and 4-Pyrrolyl-3,5-di(2-pyridyl)-4*H*-1,2,4-triazoles

Jonathan A. Kitchen,[†] Andy Noble,[†] Carsten D. Brandt,[†] Boujemaa Moubaraki,[‡] Keith S. Murray,[‡] and Sally Brooker*[,†]

Department of Chemistry and MacDiarmid Institute of Advanced Materials and Nanotechnology, University of Otago, P.O. Box 56, Dunedin, New Zealand, and School of Chemistry, Building 23, Monash University, Clayton, Victoria 3800, Australia

Received June 6, 2008

The first dinuclear iron(II) complexes of any 4-substituted 3,5-di(2-pyridyl)-4*H*-1,2,4-triazole ligands, $[Fe^{II}_2(\mathbf{adpt})_2(H_2O)_{1.5}(CH_3CN)_{2.5}](BF_4)_4$ and $[Fe^{II}_2(\mathbf{pldpt})_2(H_2O)_2(CH_3CN)_2](BF_4)_4$, are presented [where **adpt** is 4-amino-3,5-di(2-pyridyl)-4*H*-1,2,4-triazole and **pldpt** is 4-pyrrolyl-3,5-di(2-pyridyl)-4*H*-1,2,4-triazole]. Both dinuclear complexes feature doubly triazole bridged iron(II) centers that are found to be [high spin-high spin] at all temperatures, 4−300 K, and to exhibit weak antiferromagnetic coupling. In the analogous monometallic complexes, $[Fe^{II}(\mathbf{Rdpt})_2(X)_2]^{n+}$, the spin state of the iron(II) center was controlled by appropriate selection of the axial ligands X. Specifically, both of the chloride complexes, $[Fe^{II}(\mathbf{adpt})_2(Cl)_2]\cdot 2MeOH$ and $[Fe^{II}(\mathbf{pldpt})_2(Cl)_2]\cdot 2MeOH\cdot H_2O$, were found to be high spin whereas the pyridine adduct $[Fe^{II}(\mathbf{adpt})_2(py)_2](BF_4)_2$ was low spin. Attempts to prepare $[Fe^{II}(\mathbf{pldpt})_2(py)_2](BF_4)_2$ and the dinuclear analogues $[Fe^{II}_2(\mathbf{Rdpt})_2(py)_4](BF_4)_4$ failed, illustrating the significant challenges faced in attempts to develop control over the nature of the product obtained from reactions of iron(II) and these bis-bidentate ligands.

Introduction

The use of triazole and triazolate based ligands in conjunction with iron(II) is of considerable interest because of the possibility of generating magnetically interesting complexes, specifically complexes that exhibit spin crossover (SCO).[1−16] While to date the majority of these complexes have been mononuclear or polymeric, currently one key drive is toward preparing discrete polynuclear complexes to (a) probe the possible relationship between exchange coupling and SCO and (b) generate, in a controlled way, complexes exhibiting multiple SCO events, preferably with hysteresis (facilitated by communication between the metal ions), as these offer the longer term possibility of more dense information storage.[1−3,17−20]

In recent years, 4-substituted 3,5-di(2-pyridyl)-4*H*-1,2,4-triazole ligands (Figures 1 and 2) have been of particular interest to our group as they fit the above criteria, in that they are known to induce SCO in iron(II),[4−11] and they have two metal binding sites so should allow access to dinuclear

* To whom correspondence should be addressed. E-mail: sbrooker@chemistry.otago.ac.nz.
† University of Otago.
‡ Monash University.

(1) Kahn, O.; Codjovi, E. *Philos. Trans. R. Soc. London, Ser. A* **1996**, *354*, 359–379.
(2) Kahn, O. *Chem. Br.* **1999**, *2*, 24–27.
(3) Haasnoot, J. G. *1,2,4-Triazoles as ligands for iron(II) high spin-low spin crossovers*; Kluwer Academic Publishers: Dordrecht, 1996; p 299−321.
(4) Kunkeler, P. J.; van Koningsbruggen, P. J.; Cornelissen, J. P.; van der Horst, A. N.; van der Kraan, A. M.; Spek, A. L.; Haasnoot, J. G.; Reedijk, J. *J. Am. Chem. Soc.* **1996**, *118*, 2190–2197.
(5) Moliner, N.; Muñoz, M. C.; van Koningsbruggen, P. J.; Real, J. A. *Inorg. Chim. Acta* **1998**, *274*, 1–6.
(6) Moliner, N.; Muñoz, M. C.; Letard, S.; Letard, J.-F.; Solans, X.; Burriel, R.; Castro, M.; Kahn, O.; Real, J. A. *Inorg. Chim. Acta* **1999**, *291*, 279–288.
(7) Moliner, N.; Gaspar, A. B.; Muñoz, M. C.; Niel, V.; Cano, H.; Real, J. A. *Inorg. Chem.* **2001**, *40*, 3986–3991.
(8) Matouzenko, G. S.; Boussekou, A.; Borshch, S.; Perrin, M.; Zein, S.; Salmon, L.; Molnar, G.; Lecocq, S. *Inorg. Chem.* **2004**, *43*, 227–236.
(9) Shakir, M.; Parveen, S.; Begum, N.; Azim, Y. *Polyhedron* **2003**, *22*, 3181–3186.
(10) Shakir, M.; Parveen, S.; Begum, N.; Chingsubam, P. *Transition Met. Chem.* **2004**, *29*, 196–199.
(11) Zhu, D.; Xu, Y.; Yu, Z.; Guo, Z.; Sang, H.; Liu, T.; You, X. *Chem. Mater.* **2002**, *14*, 838–843.
(12) Tong, M.-L.; Tong, Y.-X.; Chen, J.-C.; Hu, S.; Zhou, A.-J. *Z. Anorg. Allg. Chem.* **2006**, (632), 475–481.
(13) Schneider, C. J.; Cashion, J. D.; Moubaraki, B.; Neville, S. M.; Batten, S. R.; Turner, D. R.; Murray, K. S. *Polyhedron* **2007**, *26*, 1764–1772.
(14) Klingele, M. H.; Moubaraki, B.; Cashion, J. D.; Murray, K. S.; Brooker, S. *Chem. Commun.* **2005**, 987–989.
(15) Kitchen, J. A.; Brooker, S. *Coord. Chem. Rev.* **2008**, *252*, 2072−2092.
(16) Grunert, C. M.; Reiman, S.; Spiering, H.; Kitchen, J. A.; Brooker, S.; Gütlich, P. *Angew. Chem., Int. Ed.* **2008**, *47*, 2997–2999.

10.1021/ic801039j CCC: $40.75
Published on Web 09/23/2008

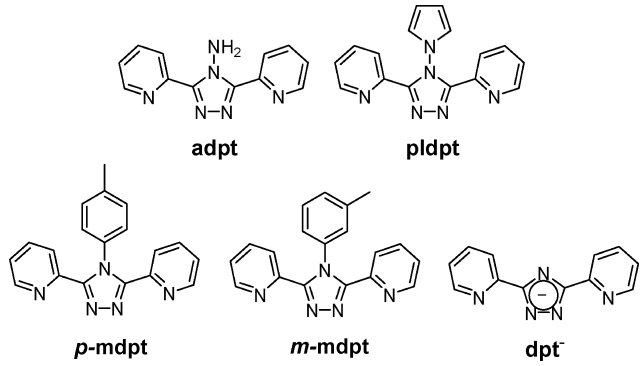

Figure 1. The only 4-substituted 3,5-di(2-pyridyl)-4*H*-1,2,4-triazole ligands used, to date, to prepare iron(II) complexes.

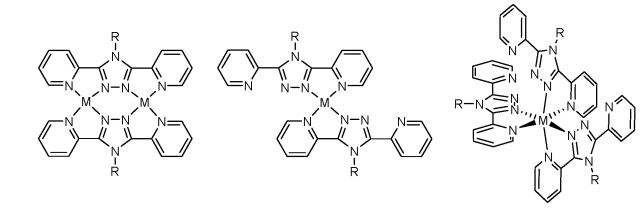

Figure 2. Three binding modes of 4-substituted 3,5-di(2-pyridyl)-4*H*-1,2,4-triazole ligands that are pertinent to this work.

complexes. In addition, the adjacent N^1N^2 triazole nitrogen atoms allow the central triazole moiety to bridge the metal centers and mediate magnetic exchange between them. However, the presence of the two bidentate binding pockets in these ligands provides a number of possible binding modes, not all of which result in dinuclear complexes.[15,21] The binding modes which are pertinent to this article are the dinuclear $(N',N^1,N^2,N'')_2$ double bridging (dinuclear bis complex), mononuclear $(N',N^1)_2$ (mononuclear bis complex), and mononuclear $(N',N^1)_3$ (mononuclear tris, Figure 2).

A selection of 4-substituted 3,5-di(2-pyridyl)-4*H*-1,2,4-triazole ligands is shown in Figure 1. Such ligands have been utilized to form a vast array of complexes with various transition metal ions [Cu(II), Co(II), Ni(II), Zn(II), Ag(I), Fe(II)] with a variety of coligands, mostly resulting in mononuclear and dinuclear complexes, but also in some complexes of other nuclearities.[21] These studies clearly establish the versatility of such ligands. One of the key advantages of this ligand family is that the substituents at the C^3, C^5, and N^4 positions are readily varied.[22] In particular, we have focused on exploring the effect that the N^4-substituent has on the nuclearity of the resulting complex, as well as on its solubility, structure (including intermolecular packing interactions), and properties.[23−25] In the case of iron(II) complexes it is possible that the electronic properties of the N^4-substitutent (electron donating or withdrawing, by resonance and/or inductive effects) will influence the ligand field strength and hence the nature of the SCO properties of the resulting iron(II) complex. In this context it is interesting to note that, prior to our work, the use of such 4-substituted 3,5-di(2-pyridyl)-4*H*-1,2,4-triazole ligands in iron(II) containing complexes has been limited to just four N^4-substituents (ligands **dpt**$^-$, **adpt**, ***m*-mdpt**, ***p*-mdpt**, Figure 1) and all of the complexes isolated have been of the mononuclear variety.[4−11,15] Herein we present the first examples of dinuclear iron(II) complexes of any 4-substituted 3,5-di(2-pyridyl)-4*H*-1,2,4-triazole ligands, $[Fe^{II}_2(\mathbf{adpt})_2(H_2O)_{1.5}(CH_3CN)_{2.5}](BF_4)_4$ and $[Fe^{II}_2(\mathbf{pldpt})_2(H_2O)_2(CH_3CN)_2](BF_4)_4$. In addition, we demonstrate that choice of reaction stoichiometry is not sufficient to control the nature of the iron(II) product obtained, for example mononuclear bis versus mononuclear tris versus dinuclear bis (Figure 2). Some mononuclear bis complexes of these ligands, $[Fe^{II}(\mathbf{adpt})_2(Cl)_2]$, $[Fe^{II}(\mathbf{pldpt})_2(Cl)_2]$, and $[Fe^{II}(\mathbf{adpt})_2(py)_2](BF_4)_2$ are also described. A discussion of the synthetic challenges, crystal structures, and magnetic properties of these complexes is presented.

Results and Discussion

Synthesis of Iron(II) Complexes of Rdpt. Two N^4-substituted 3,5-di(2-pyridyl)-4*H*-1,2,4-triazole ligands, **adpt** and **pldpt** (Figure 2), prepared as previously described,[24,26,27] have been reacted with various iron(II) salts in different stoichiometric ratios and solvent systems to test our control over the nature, in particular the nuclearity and axial substituents, of the products. All reactions were carried out in air; no precautions to exclude air or moisture were found to be necessary.

A stoichiometric reaction between the appropriate ligand and iron(II) chloride tetrahydrate in methanol (Scheme 1) gave the 1:2 mononuclear complexes $[Fe^{II}(\mathbf{adpt})_2(Cl)_2]$ and $[Fe^{II}(\mathbf{pldpt})_2(Cl)_2]$. The complexes were isolated as relatively large, orange, single crystals by vapor diffusion of diethyl ether into the orange-red reaction solutions. Single crystal X-ray structure determinations were carried out on both complexes (see below), confirming the anticipated mononuclear bis binding mode of the ligands (Figure 2), with axial chloride groups completing the octahedral N_4Cl_2 coordination sphere. After drying in air, the complexes lost some of the methanol and/or water molecules of crystallization, yielding bulk samples of $[Fe^{II}(\mathbf{adpt})_2(Cl)_2]\cdot 1.5MeOH\cdot 1.5H_2O$ and $[Fe^{II}(\mathbf{pldpt})_2(Cl)_2]\cdot 2MeOH\cdot H_2O$, in 36 and 68% yield, respectively.

(17) Gaspar, A. B.; Muñoz, M. C.; Real, J. A. *J. Mater. Chem.* **2006**, (16), 2522–2533.
(18) Breuning, E.; Ruben, M.; Lehn, J.-M.; Renz, F.; Garcia, Y.; Ksenofontov, V.; Gütlich, P.; Wegelius, E.; Rissanen, K. *Angew. Chem., Int. Ed.* **2000**, *39*, 2504–2507.
(19) Ruben, M.; Breuning, E.; Lehn, J.-M.; Ksenofontov, V.; Renz, F.; Gütlich, P.; Vaughan, G. B. M. *Chem.—Eur. J.* **2003**, *9*, 4422–4429.
(20) Letard, J.-F.; Guionneau, P.; Capes, L. *Top. Curr. Chem.* **2004**, *235*, 221–249.
(21) Klingele, M. H.; Brooker, S. *Coord. Chem. Rev.* **2003**, *241*, 119–132.
(22) Klingele, M. H.; Brooker, S. *Eur. J. Org. Chem.* **2004**, *342*, 2–3434.
(23) Klingele, M. H.; Boyd, P. D. W.; Moubaraki, B.; Murray, K. S.; Brooker, S. *Eur. J. Inorg. Chem.* **2005**, 910–918.
(24) Klingele, M. H.; Boyd, P. D. W.; Moubaraki, B.; Murray, K. S.; Brooker, S. *Eur. J. Inorg. Chem.* **2006**, 573–589.
(25) Klingele, M. H.; Noble, A.; Boyd, P. D. W.; Brooker, S. *Polyhedron* **2007**, *26*, 479–485.
(26) Geldard, J. F.; Lions, F. *J. Org. Chem.* **1965**, *30*, 318–319.
(27) Mandal, S. K.; Clase, H. J.; Bridson, J. N.; Ray, S. *Inorg. Chim. Acta* **1993**, *209*, 1–4.

Scheme 1. Synthesis of Mononuclear and Dinuclear Complexes of the Bis-bidentate Triazole Ligands **adpt** and **pldpt**[a]

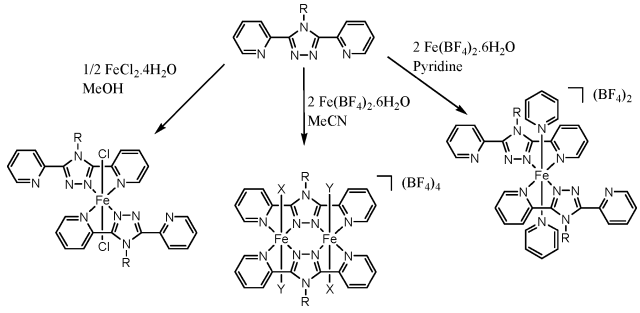

[a] R = NH_2, pyrrolyl; X = H_2O; Y = CH_3CN.

In contrast, an attempt to access the 2:2 complexes $[Fe^{II}_2(\mathbf{adpt})_2(Cl)_4]$ and $[Fe^{II}_2(\mathbf{pldpt})_2(Cl)_4]$ by the stoichiometric reaction of 2 equiv of $FeCl_2 \cdot 4H_2O$ with the respective ligand, in methanol, resulted only in the aforementioned 1:2 products. These 2:2 reactions were therefore repeated with the non-coordinating BF_4^- anion, rather than the coordinating chloride anion, in the hope that this might facilitate access to dinuclear complexes $[Fe^{II}_2(\mathbf{Rdpt})_2(X)_4](BF_4)_4$ where X = solvent molecule. However, it resulted in a mixture of the desired dinuclear complexes and the mononuclear 1:3 products, $[Fe^{II}(\mathbf{Rdpt})_3](BF_4)_2$.[28] To obtain clean samples of the 2:2 complexes of interest, $[Fe^{II}_2(\mathbf{adpt})_2(X)_4](BF_4)_4$ and $[Fe^{II}_2(\mathbf{pldpt})_2(X)_4](BF_4)_4$, an excess of iron(II) was required to suppress formation of the tris complexes. Specifically, the reaction of 2 equiv of iron(II) tetrafluoroborate hexahydrate with 1 equiv of the appropriate ligand, **adpt** and **pldpt**, in acetonitrile was employed (Scheme 1). This resulted in orange-red solutions which upon vapor diffusion of diethyl ether resulted in the formation of yellow block crystals. Upon removal of these crystals from the diethyl ether/acetonitrile mother liquor and air drying, they cracked and lost their luster, resulting in yellow solids. The microanalysis results obtained on these air-dried samples were consistent with the formulae $[Fe^{II}_2(\mathbf{adpt})_2(H_2O)_4](BF_4)_4$ and $Fe^{II}_2(\mathbf{pldpt})_2(H_2O)_4$-MeCN $(BF_4)_4$. They were obtained in 28 and 23% yield, respectively. These samples were used for the bulk magnetism and infrared studies. In contrast, the structure determinations carried out on the single crystals (see below) indicated that in both complexes the axial ligands were a mixture of MeCN and H_2O.

While the successful preparation of these, the first such dinuclear complexes, is a significant breakthrough, both of them contain an O-donor in the iron(II) coordination sphere and this is not favorable if one is aiming for SCO [for iron(II) an N_6 environment is the best bet]. Hence, consideration was given to developing access to dinuclear iron(II) complexes in which both iron(II) centers had N_6 coordination spheres. With the observations that (a) in the presence of coordinating counteranions, such as chloride (see above) and thiocyanate/selenocyanate/TCNQ/dicyanamide,[15] neutral mononuclear (1:2) complexes tend to form regardless of stoichiometry, and (b) in the presence of non-coordinating anions, when the metal salt is present in excess, dinuclear complexes with axial solvent molecules are formed, it was decided to attempt the synthesis in pyridine with $Fe(BF_4)_2.6H_2O$. The reaction was carried out in a non-stoichiometric 2:1 Fe:**Rdpt** ratio to suppress formation of the tris complex. Vapor diffusion of diethyl ether into the resulting very deep red pyridine reaction solution gave two products, a pale yellowish white powder, $[Fe(pyridine)_4(H_2O)_2](BF_4)_2$, and dark red crystals which were suitable for a single crystal X-ray structure determination (see later). Interestingly this revealed that the product was actually the mononuclear 1:2 complex $[Fe^{II}(\mathbf{adpt})_2(pyridine)_2](BF_4)_2$ despite the 2:1 reaction ratio, choice of pyridine solvent, and non-coordinating counteranion. The red crystals were isolated by filtering the two compounds and washing the pale powder out with methanol, affording the red crystals in 11% yield. These crystals quickly lost their luster on drying, and the bulk sample had a microanalysis consistent with only one axial pyridine. Repeating this reaction with an even greater excess of iron (up to 20:1 Fe:**Rdpt**) did not lead to the formation of the desired dinuclear complex, $[Fe^{II}_2(\mathbf{adpt})_2(pyridine)_4](BF_4)_4$, but rather, once again, the mononuclear complex.

Comparison with Related Dimetallic Complexes. In the synthesis of dinuclear complexes of **Rdpt** ligands with other first row transition metal ions we have shown that the product obtained is strongly influenced by the reaction stoichiometry.[23−25] However, the present study shows that iron(II) does not come as close to obeying the "stoichiometry rules" with which the other first row transition metal ions appear to be fairly compliant. Other factors, such as the relative solubilities of the various possible products in the chosen solvent(s), may also influence the outcome of a given reaction,[25] but it is likely that a key additional factor in the case of iron(II) is the spin state of the iron(II) center in the various possible reaction products, with low spin (LS) products generally favored over high spin (HS) ones. Indeed, this is believed to be the reason for the frequent observation of some LS 1:3, mono tris (Figure 1), product, a problem that has been minimized by loading the solution with iron(II). However, despite the fact that the desired dinuclear complex $[Fe^{II}_2(\mathbf{adpt})_2(pyridine)_4](BF_4)_4$ is anticipated to be [LS-LS] at room temperature, despite many attempts, it has not yet been isolated. This is intriguing as $[Fe^{II}_2(\mathbf{Rdpt})_2(H_2O)_2(CH_3CN)_2](BF_4)_4$, where **Rdpt** is **adpt** or **pldpt**, complexes have been isolated, indicating once again that there are no major steric problems destabilizing the desired, doubly bridged, dinuclear product in favor of mononuclear products. However, both of these complexes are [HS-HS] from 4 to 300 K so the iron(II) centers are geometrically flexible. All in all, it appears that the presence of two, geometrically demanding, LS iron centers may be disfavoring the formation of the desired dinuclear doubly triazole-bridged complex, relative to the observed LS mononuclear iron(II) complex, $[Fe^{II}(\mathbf{adpt})_2(pyridine)_2](BF_4)_2$, that is, the [LS-LS] dimetallic complex appears to be energetically unfavorable relative to the [LS] monometallic complex so it does not form with these low denticity, bis-bidentate, ligands. This contrasts with the situation seen for diiron(II) bis[3,5-di(2-pyridyl)-1,2-

(28) Kitchen, J. A.; White, N. G.; Boyd, M.; Moubaraki, B.; Murray, K. S.; Boyd, P. D. W.; Brooker, S. manuscript in preparation.

pyrazolates),[13,29,30] most probably because those complexes are prepared and isolated as [HS-HS] complexes that usually convert to [LS-LS] species at low temperatures, but is somewhat similar to the diiron(II) complex of the bis-terdentate triazole ligand PMAT, $[Fe^{II}_2(PMAT)_2](BF_4)_4\cdot$ DMF, in that the [HS-HS] complex can, on lowering the temperature below 224 K, be converted to the [HS-LS] complex;[14,16] however, even under high pressures (10.3 kBar) and low temperatures (4 K), the complex never converts to the [LS-LS] form.[31] In summary, it seems likely that the use of a slightly weaker ligand field axial ligand than pyridine might allow the *isolation of an SCO active dinuclear complex in the [HS-HS] state* and only then to establish access, at lower temperatures, to the half SCO state and perhaps also the [LS-LS] state.

X-ray Crystal Structures. All X-ray crystal structure data were obtained at low temperatures (83−93 K). Orange block crystals of $[Fe^{II}(\mathbf{adpt})_2(Cl)_2]\cdot$2MeOH were grown from methanol by vapor diffusion of diethyl ether and the X-ray crystal structure determined (Figure 3, Tables 1 and 2). The asymmetric unit is made up of one half of the molecule with the other half being generated by a center of inversion located at the iron(II) center. The iron(II) center has an octahedral geometry with two $(N',N^1)_2$ coordinated (i.e., bound via the pendant pyridyl nitrogen and one of the two adjacent triazole nitrogens) **adpt** ligands occupying the equatorial positions and two unidentate *trans*-coordinated chlorides at the apical sites. The bond lengths and angles are consistent with those expected for a HS iron(II) center (Table 1). The $Fe-N_{pyrid}$ bond length, 2.1899(16) Å, is slightly longer than the $Fe-N_{triaz}$ bond length, 2.1379(16) Å. As expected, the axial Fe−Cl bonds are even longer, 2.4551(5) Å.

The **adpt** ligand is fairly flat, with just a small angle between the central triazole ring and the coordinated pyridine ring [7.94(15)°] and the non-coordinated pyridine ring [8.79(14)°]. As expected, the non-coordinated pyridine ring has its nitrogen atom, N(4), facing away from the iron center. This reduces the electrostatic repulsion between N(3) and N(4) and facilitates hydrogen bonding between a hydrogen atom on the N(6) amino N^4-substituent and N(4) [N(6)···N(4) = 2.894(3) Å; N(6)−H(6A)−N(4) = 116°]. The amino substituent, N(6), is also hydrogen bonded to the oxygen atom of the methanol of solvation [N(6)···O(20)′ = 2.958(3) Å; N(6)−H(6B)−O(20)′ = 176°] within the crystal lattice. The methanol hydroxyl group is in turn hydrogen bonded to the coordinated chloride atom [O(20)···Cl(1) = 3.085(3) Å; O(20)−H(20)−Cl(1) = 158°]. The cations are linked not only via this hydrogen bonding network but also through π-π interactions. Layers of stepped cations are formed by each **adpt** ligand forming a pair of π-π interactions between the triazole ring on one cation and the non-coordinated pyridine ring on the next cation [Supporting Information, Figure S1; centroid···centroid = 3.6834(16) Å]. These π-π linked stepped layers are linked to neighboring π-π linked stepped layers via the hydrogen bonding methanol molecule, O(20), mentioned previously. The O(20) methanol molecule interacts with one layer via the O(20)−H(20)···Cl(1) hydrogen bond and with the adjacent layer via the N(6)′−H(6B)′···O(20) hydrogen bond. Running perpendicular to these stepped layers is a second series of identically π-π stacked stepped molecules (Supporting Information, Figure S2). The overall result is an efficiently packed array of interacting complexes (Supporting Information, Figure S3).

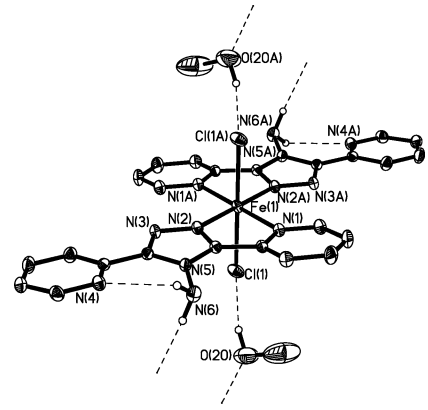

Figure 3. Perspective view of the complex $[Fe^{II}(\mathbf{adpt})_2(Cl)_2]\cdot$2MeOH (hydrogen atoms other than those on O or N are omitted for clarity).

Single crystals of $[Fe^{II}(\mathbf{pldpt})_2(Cl)_2]\cdot$2MeOH·$H_2O$ were grown by the same method as for the **adpt** analogue. This complex (Figure 4, Tables 1 and 2) is isostructural, but not isomorphous, to $[Fe^{II}(\mathbf{adpt})_2(Cl)_2]\cdot$2MeOH. The octahedral iron(II) center is coordinated in the same $(N',N^1)_2$ fashion to two **pldpt** ligands in the equatorial plane and to two *trans* chloride anions. Only half of the complex is present in the asymmetric unit; the other half is generated by a center of inversion located at the iron(II) center. Again the bond lengths and angles are consistent with those expected for a HS iron(II) center (Table 1). As before, the $Fe-N_{pyrid}$ bond length [2.1882(12) Å] is slightly longer than the $Fe-N_{triaz}$ bond length [2.1396(11) Å], and the axial Fe−Cl bonds are the longest [2.4560(6) Å].

The dipyridyl triazole portion of the **pldpt** ligand is also fairly flat [angle between the central triazole ring and the coordinated pyridyl ring is 8.75(10)°; the non-coordinated pyridyl ring, 9.49(11)°] and the non-coordinated pyridyl ring again has the nitrogen atom facing away from the iron center, facilitating hydrogen bonding to N(6). The pyrrolyl ring is almost perpendicular to that of the triazole, 79.10(6)°, so

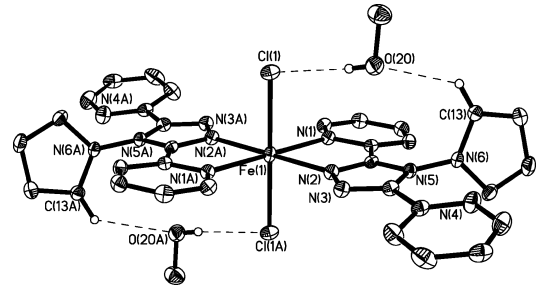

Figure 4. Perspective view of the complex $[Fe^{II}(\mathbf{pldpt})_2(Cl)_2]\cdot$2MeOH·$H_2O$ (hydrogen atoms other than those on O, and severely disordered H_2O, are omitted for clarity).

(29) Nakano, K.; Kawata, S.; Yoneda, K.; Fuyuhiro, A.; Yagi, T.; Nasu, S.; Morimoto, S.; Kaizaki, S. *Chem. Commun.* **2004**, 2892–2893.
(30) Kaizaki, S.; Nakano, K.; Suemura, N.; Yoneda, K.; Kawata, S. *Dalton Trans.* **2005**, 740–743.
(31) Bhattacharjee, A.; Ksenofontov, V.; Kitchen, J. A.; White, N. G.; Brooker, S.; Gütlich, P. *Appl. Phys. Lett.* **2008**, *92*, 174104.

Table 1. Summary of Iron(II) Bond Lengths and Angles in the Mononuclear and Dinuclear Complexes[a]

	$[Fe^{II}(\mathbf{adpt})_2(Cl)_2]\cdot 2MeOH$[#1]	$[Fe^{II}(\mathbf{pldpt})_2(Cl)_2]\cdot 2MeOH\cdot H_2O$[#2]	$[Fe^{II}_2(\mathbf{pldpt})_2(H_2O)_2(CH_3CN)_2](ClO_4)_4$[#3]	$[Fe^{II}_2(\mathbf{pldpt})_2(H_2O)_2(CH_3CN)_2](BF_4)_4$[#4]	$[Fe^{II}(\mathbf{adpt})_2(py)_2](BF_4)_2\cdot 2.4py\cdot 0.6Et_2O$
$Fe-N_{py}$	2.1899(16)	2.1882(11)	2.2536(16)	2.2390(13)	2.0094(19)
$Fe-N_{Triaz}$	2.1379(16)	2.1396(12)	2.1343(16)	2.1293(12)	1.9560(19)
$Fe-X$[b]	2.4551(5)[#a]	2.4560(6)[#a]	2.1303(17)[#b]	2.1274(13)[#b]	1.9983(19)[#d]
$Fe-N_{py}$[c]			2.2173(16)	2.2119(12)	2.0108(19)
$Fe-N_{Triaz}$[c]			2.1555(16)	2.1487(12)	1.9654(19)
$Fe-X$[b,c]			2.0836(15)[#c]	2.0850(12)[#c]	2.0037(19)[#d]
cis bond angle range	75.78(6)−104.22(6)	75.88(4)−104.12(4)	73.98(6)−121.38(6)	74.26(5)−121.40(5)	80.31(8)−99.99(8)
trans bond angle range	N/A	N/A	163.85(6)−169.31(7)	163.59(5)−170.35(5)	178.08(7)−179.76(8)
intramolecular Fe···Fe	N/A	N/A	4.389	4.391	N/A

[a] Symmetry transformations used to generate equivalent atoms: [#1] $= -x, -y+1, -z$; [#2] $= -x+1, -y+1, -z+1$; [#3] $= -x+1, -y+1, -z+1$; [#4] $= -x+1, -y+1, -z+1$. [b] [#a] X = Cl; [#b] X = MeCN; [#c] X = H_2O; [#d] X = pyridine. [c] Entries in this row are present only for complexes for which there are six independent bonds to iron.

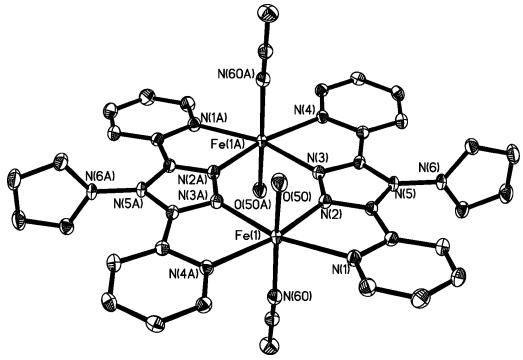

Figure 5. Perspective view of the $[Fe^{II}_2(\mathbf{pldpt})_2(H_2O)_2(CH_3CN)_2]^{4+}$ cation (hydrogen atoms are omitted for clarity).

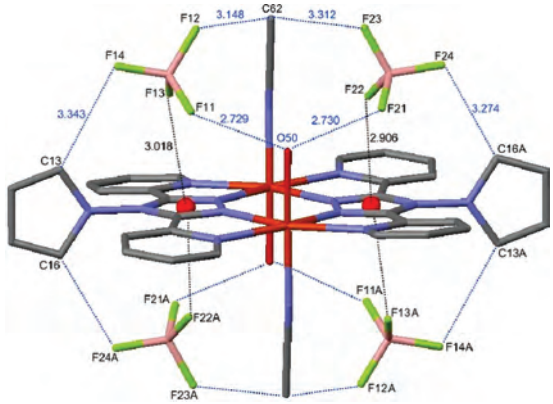

Figure 6. Perspective view of $[Fe^{II}_2(\mathbf{pldpt})_2(CH_3CN)_2(H_2O)_2](BF_4)_2$ showing hydrogen bonding interactions (in blue) and anion-π interactions (in black). Hydrogen atoms and symmetry generated BF_4^- counteranions have been omited for clarity.

this should prevent π-mediated electronic interactions between them. As in the previous structure, the methanol molecule of solvation is hydrogen bonded to the coordinated chloride [O(20)···Cl(1) = 3.1660(14) Å and O(20)−H(20)−Cl(1) = 176°]. In addition to this there is also a weak C−H···O hydrogen bond to a C−H group on the pyrrolyl N^4-substituent [C(13)···O(20) = 3.286 Å and C(13)−H(13)−O(20) = 133°; Supporting Information, Figure S4]. These two hydrogen bonds position the methanol such that it is in close proximity to the centroid of the triazole ring [O(20)··· centroid = 3.0422(15) Å]. The packing is not discussed in detail as the SQUEEZE routine of PLATON[32] was used to deal with what appeared to be a severely disordered water molecule of solvation.

Yellow block shaped crystals of $[Fe^{II}_2(\mathbf{pldpt})_2(H_2O)_2(CH_3CN)_2](BF_4)_4$ were grown from acetonitrile by vapor diffusion of diethyl ether. The structure contains two triazole ligands bridging two iron(II) centers. The iron centers are crystallographically identical as the complex crystallizes in the space group $P\bar{1}$ with the iron atoms related through the center of inversion (Figure 5). The bond lengths and angles are consistent with those expected for a HS iron(II) center (Table 1). As in the structure of $[Fe^{II}(\mathbf{pldpt})_2Cl_2]$ the pyrrolyl ring is twisted at near right angles with respect to the triazole ring, 88.42(6)°.

Two strong, and almost identical, classical hydrogen bonds exist in this complex, both involving the coordinated water molecule as the donor and the tetrafluoroborate fluorine atoms as the acceptors [O(50)···F(11) = 2.7290(17) Å and O(50)−H(50A)−F(11) = 165°; O(50)···F(21) = 2.7296(16) Å and O(50)−H(50B)−F(21) = 165°]. The BF_4^- counterions also exhibit some non classical, and weaker, C−H···F hydrogen bonds. The intramolecular C−H···F interactions involve the axially coordinated acetonitrile methyl group [C(62)···F(12) = 3.148(2) Å and C(62)−H(62C)−F(12) = 137°; and C(62)···F(23) = 3.312(2) Å and C(62)−H(62A)−F(23) = 173°] and the pyrrolyl headgroup carbon atoms [C(13)···F(14) = 3.274(2) Å and C(13)−H(13)−F(14) = 156°; and C(16)···F(24) = 3.343(2) Å and C(16)−H(16)−F(24) = 157°]. The intermolecular C−H···F interactions facilitate the linking of adjacent cations: the BF_4^- labeled F(11)−F(14) interacts with a C−H group on a pyridine ring [C(1)···F(14) = 3.221 Å and C(1)−H(1)−F(14) = 135°], while the BF_4^- labeled F(21)−F(24) interacts with a methyl C−H on an adjacent, axially bound, acetonitrile [C(62)···F(22) = 3.096(2) Å and C(62)−H(62B)−F(22) = 146°].

There are also strong anion···π (strictly anion···π*) interactions[33] from the fluorine atoms to the π-acidic triazole ring. Each triazole ring in $[Fe^{II}_2(\mathbf{pldpt})_2(H_2O)_2(CH_3CN)_2](BF_4)_4$ makes two anion···π interactions, one to each of the BF_4^- anions [centroid···F distances of 3.018 and 2.906 Å, respectively; symmetry dictates that each triazole ring has an identical pair of these interactions] (Figure 6). The perchlorate analogue of this complex was prepared and

(32) van der Sluis, P.; Spek, A. L. *Acta Crystallogr., Sect. A* **1990**, *46*, 194–201.
(33) Schottel, B. L.; Chifotides, H. T.; Dunbar, K. R. *Chem. Soc. Rev.* **2008**, *37*, 68–83.

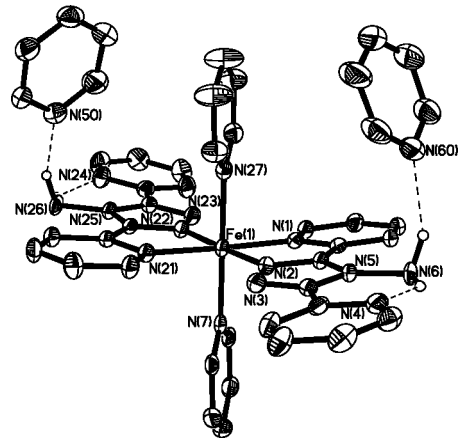

Figure 7. Perspective view of $[Fe^{II}(\mathbf{adpt})_2(py)_2]^{2+}\cdot 2py\cdot$ (tetrafluoroborate counteranions, partial occupancy solvent, and hydrogen atoms, except those on amino groups, are omitted for clarity).

shown, by X-ray structure determination, to be isomorphous (Supporting Information, Figure S5).

The slow diffusion of diethyl ether vapor into the acetonitrile reaction solution gave yellow crystals of $[Fe^{II}_2(\mathbf{adpt})_2(H_2O)_{1.5}(CH_3CN)_{2.5}](BF_4)_4$. A poor quality X-ray data set was obtained and confirmed that the connectivity of the complex was the same as that of $[Fe^{II}_2(\mathbf{pldpt})_2(H_2O)_2(CH_3CN)_2](BF_4)_4$; however, no detailed structural analysis can be presented (Supporting Information, Figure S6).

Vapor diffusion of diethyl ether into the pyridine reaction solution gave red single crystals of $[Fe^{II}(\mathbf{adpt})_2(py)_2](BF_4)_2\cdot 2.4py\cdot 0.6Et_2O$ suitable for an X-ray structure determination. This revealed that, despite the 2:2 Fe/**adpt** reaction ratio, the desired dinuclear product had not formed, rather the mononuclear variant $[Fe^{II}(\mathbf{adpt})_2(py)_2](BF_4)_2\cdot 2.4py\cdot 0.6Et_2O$ was obtained (Figure 7). This complex has a similar overall structure to the previous mononuclear complexes (albeit with axial Cl^-); however, in this case there is no crystallographic symmetry within the complex and it is cationic with the 2+ charge balanced by two tetrafluoroborate counteranions. The asymmetric unit also contains two full occupancy and a 0.4 occupancy pyridine molecule of solvation, with a 0.6 occupancy diethyl ether sharing the same position as the 0.4 occupancy pyridine in the crystal lattice and also sharing a carbon atom. In contrast to all of the previous structures, the bond lengths and angles are consistent with those expected for a *LS iron(II) center* (Table 1). Although the individual ligands in this complex are relatively planar (1.8−6.0° angle between triazole and pyridyl ring mean planes), the cation as a whole displays a bowed configuration, with both ligands bent down somewhat relative to the equatorial plane (Figure 8). This can be rationalized by analyzing the hydrogen bonding interactions. Each of the amino 4-substituents is involved in two hydrogen bonds, the first (which is seen in most complexes of this ligand) is between the amino groups and the uncoordinated pyridine nitrogen atoms [N(6)···N(4) = 2.846(3) Å and N(6)−H(6X)···N(4) = 139°] and [N(26)···N(24) = 2.844(3) Å and N(26)−H(26Y)···N(24) = 141°]. The second interaction, and the one potentially responsible for the bowing effect, occurs between both amino head groups and the nitrogen atoms on the two full occupancy pyridines of solvation (one pyridine

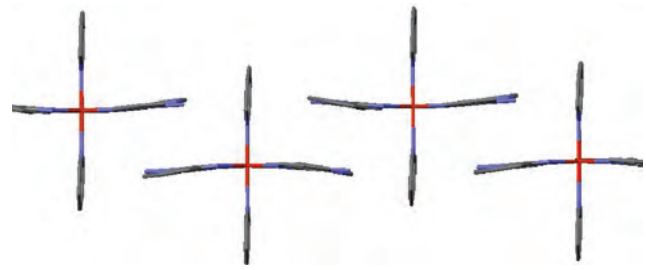

Figure 8. View of the $[Fe^{II}(\mathbf{adpt})_2(py)_2]^{2+}$ packing arrangement showing the bowing of the triazole ligands with respect to the equatorial plane (viewed edge on, running horizontally).

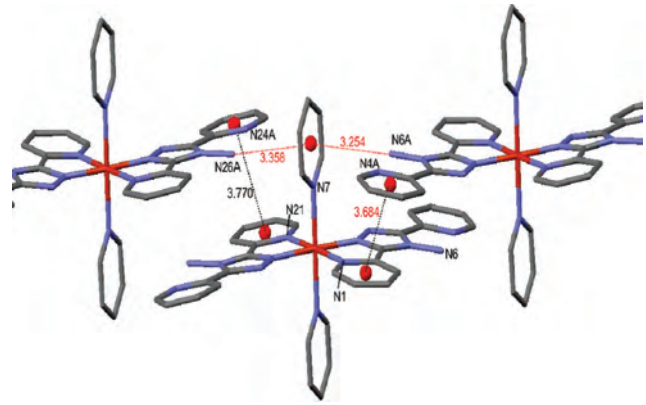

Figure 9. Perspective view of packing interactions in $[Fe^{II}(\mathbf{adpt})_2(py)_2]^{2+}$ showing the π-π interactions (in black) and the amino headgroup short contacts (in red).

per amino group) [N(6)···N(60) = 2.943(3) Å and N(6)−H(6Y)···N(60) = 155°; N(26)···N(50) = 2.920(3) Å and N(26)−H(26Y)···N(50) = 156°]. These second hydrogen bonds are both on the same side of the cation, with respect to the equatorial plane, thus facilitating the bowing by constraining one side of the molecule. Other packing interactions may help to facilitate this observed bowing, including π-π stacking interactions (Figure 9). These involve the triazole pyridine rings, such that there is an interaction between the coordinated pyridine ring of N(1) and the uncoordinated pyridine ring of N(4) on the adjacent cation [centroid−centroid = 3.684(2) Å]. There is a similar interaction between the coordinated pyridine of N(21) and the uncoordinated ring of N(24) [centroid−centroid = 3.684(2) Å]. These π-π interactions position the amino headgroup such that they appear to have short contacts to the axially coordinated pyridine rings [N(6)···centroid = 3.254(2) Å and N(26)···centroid = 3.358(2) Å] (Figure 9). These interactions bring the cations into close proximity; thus deformation of planarity may occur to allow the π interactions between ligand rings, hence further stabilizing this bowing effect. The structure also exhibits anion-π interactions. One fluorine atom from each part of the disordered tetrafluoroborate counteranion is involved in a B−F···π interaction to the uncoordinated pyridine ring of N(4) [F(24)···centroid = 3.108(4) Å and F(28)···centroid = 3.19(2) Å; F(24):F(28) 0.75:0.25 occupancy].

Magnetic Properties. As expected, given the low ligand field strength of chloride ions, the magnetic profiles of the two mononuclear complexes $[Fe^{II}(\mathbf{adpt})_2(Cl)_2].2MeOH$ and $[Fe^{II}(\mathbf{pldpt})_2(Cl)_2].MeOH\cdot H_2O$ confirmed that they were HS throughout the temperature range studied (4−300 K).

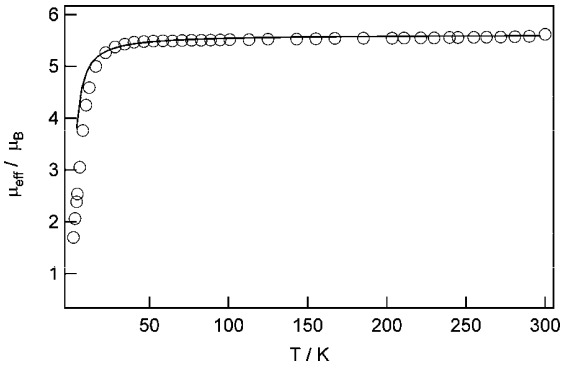

Figure 10. Plot of μ_{eff} (BM) vs temperature (K) for $[Fe^{II}_2(\mathbf{pldpt})_2(H_2O)_2(CH_3CN)_2](BF_4)_4$. Circles are data points; solid line is the best-fit calculated using the parameters given in the text.

Likewise, the presence of low ligand field water molecules in the coordination spheres of the iron(II) centers in the dinuclear complexes, $[Fe^{II}_2(\mathbf{adpt})_2(H_2O)_4](BF_4)_4$ and $[Fe^{II}_2(\mathbf{pldpt})_2(H_2O)_2\ (CH_3CN)_2](BF_4)_4$, also resulted in the complexes remaining in the [HS-HS] form throughout the 4−300 K temperature range (Figure 10). $[Fe^{II}_2(\mathbf{pldpt})_2(H_2O)_2(CH_3CN)_2](BF_4)_4$ displayed very weak antiferromagnetic coupling between the iron(II) centers ($g = 2.29$, $J = -0.44$ cm^{-1}, using the $-2J\mathbf{S_1 \cdot S_2}$ Heisenberg approach that assumes orbital contribution in parent $^5T_{2g}$ Fe(II) states is quenched), as well as some weak intermolecular interactions, which is understandable based on the aforementioned interactions that link the cations in the crystal lattice. Zero-field splitting can also contribute to this decrease. In contrast to these HS complexes, the magnetic moment of $[Fe^{II}(\mathbf{adpt})_2(py)_2](BF_4)_2$ (Supporting Information, Figure S7) fell between 0.7 and 1.1 μ_B, per Fe(II), over the entire temperature range studied. This is a little higher than the usual value of about 0.7 μ_B at room temperature, expected to decrease with decreasing temperature because of its origin as a second order Zeeman temperature independent susceptibility (TIP) term in fully low-spin d^6 (t_{2g}^6) systems. Some Curie-like contribution is present in the sample that we do not believe is because it is trapped from the HS state of a SCO system, there being no marked increase in μ_{eff} at high temperatures. It is more likely that this originates from traces of a partially desolvated HS species; the pyridine of solvation is known to be readily lost. This contrasts with the neutral dichloride structures in this study and also all of the related iron(II) complexes of 4-substituted-3,5-di(2-pyridyl)-4*H*-1,2,4-triazoles as they are either HS at all temperatures studied, or display SCO,[4−11,15] but none of which have been found to be fully LS at all temperatures studied.

Conclusions

The reaction of the ligands **adpt** and **pldpt** with iron(II) chloride tetrahydrate in both a 1:1 and a 1:2 ratio resulted in the formation of the orange, neutral, mononuclear 1:2 iron(II) complexes $[Fe^{II}(\mathbf{adpt})_2(Cl)_2]\cdot 2MeOH$ and $[Fe^{II}(\mathbf{pldpt})_2(Cl)_2]\cdot\ 2MeOH\cdot H_2O$. These two ligands were also reacted with iron(II) terafluoroborate hexahydrate in a non-stoichiometric 2:1 metal to ligand ratio to give the yellow complexes $[Fe^{II}_2(\mathbf{adpt})_2(H_2O)_{1.5}(CH_3CN)_{2.5}](BF_4)_4$ and $[Fe^{II}_2(\mathbf{pldpt})_2(H_2O)_2(CH_3CN)_2](BF_4)_4$. These are the *first examples of dinuclear iron(II) complexes of any 4-substituted 3,5-di(2-pyridyl)-4H-1,2,4-triazole*. The excess of the metal salt was required as when a 2:2 ratio iron(II)/ligand ratio was employed, with the non-coordinating BF_4^- anion, the desired dinuclear complex was contaminated with the 1:3 product.[28] All four of these complexes feature axial coordination by a weak field ligand, either chloride or water, so it is not surprising that all of them were found to be HS down to 4 K.

In an attempt to generate dinuclear complexes, $[Fe^{II}_2(\mathbf{Rdpt})_2(N\text{-donor})_4](BF_4)_4$, featuring stronger field, N_6 coordination of the iron(II) centers, pyridine was used as the reaction solvent in place of acetonitrile. However, despite the 2:1 Fe/**Rdpt** ratio employed, the mononuclear 1:2 product $[Fe^{II}(\mathbf{adpt})_2(py)_2](BF_4)_2\cdot 2.4py\cdot 0.6Et_2O$, was obtained. This complex is the *first example of a bis mono complex* (Figure 2) *with neutral axial groups*; all previous examples with iron(II) have featured axially bound anions.[15] This complex was found to be LS at all temperatures 4−300 K studied, *the first such complex to be other than HS or SCO active*. This result also confirms that, as expected, the nature of the axially bound group is of key importance to the spin state.

It is clear from these studies that (a) stoichiometry does not play as dominant a role in determining the outcome of reactions involving iron(II) as it did for other first row transition metal(II) ions and (b) our understanding and control over the nature of the product formed in iron(II) complexations of 4-substituted 3,5-di(2-pyridyl)-4*H*-1,2,4-triazoles remains in its infancy. This lack of control is frustrating as dinuclear N_6-coordinated iron(II) complexes of these ligands should be of great magnetic interest as (a) N_6 environments should bring iron(II) close to SCO and (b) the bridging triazole moiety can facilitate exchange coupling, mediating communication between the two iron(II) centers which might generate sufficient intradinuclear cooperativity to lead to SCO with hysteresis. In this study we have established that access to such complexes is nontrivial but also gained some insight into the factors which are important to achieve the desired outcome; in particular, that the spin state of the "as isolated" complex may be of particular importance with regard to the possibility of isolating dinuclear iron(II) complexes.

The iron(II) complexes described herein display extensive intra- and intermolecular interactions, including hydrogen bonding, anion-π, and π-π stacking interactions. While these particular complexes do not exhibit SCO behavior this shows that this family of **Rdpt** ligands can generate communication between adjacent complexes, which can be fine-tuned by choice of N^4-substituent[22] (facilitating abrupt SCO and hysteresis once the correct ligands are employed). Our current focus is therefore on the preparation and characterization of families of (a) mononuclear tris complexes[28] and (b) mononuclear bis complexes with axial anions that often induce SCO in iron(II), specifically thiocyanate, selenocyanate, cyanoborohydride, or dicyanamide[15] (another bonus is that these axial groups are not prone to being lost, unlike the axial solvent molecules in many of the complexes described herein). Variation of the 4-substitutent of the N^4-substituted 3,5-di(2-pyridyl)-4*H*-1,2,4-triazoles, **Rdpt**, used in these

studies, across a very wide range,[22] provides us with an elegant method of manipulating both the ligand field strength experienced by the iron(II) in the resulting families of mononuclear complexes and the nature and extent of the intermolecular packing interactions.

Experimental Section

The **adpt** and **pldpt** ligands were prepared as described elsewhere.[24,26,27] $FeCl_2 \cdot 4H_2O$ and $Fe(ClO_4)_2 \cdot 6H_2O$ were purchased from Aldrich and used as received. $Fe(BF_4)_2 \cdot 6H_2O$ was purchased from Aldrich and used as received. All of the complexation reactions were carried out in air. Methanol was dried by freshly distilling over magnesium and iodine before use. Acetonitrile was dried by freshly distilling over calcium hydride before use. Elemental analyses were carried out by the Campbell Microanalytical Laboratory at the University of Otago. Infrared spectra were recorded over the range 4000−400 cm^{-1} with a Perkin-Elmer Spectrum NBX FT-IR spectrophotometer as potassium bromide pellets. Magnetic data were recorded over the range 300−4.2 K with a Quantum Design MPMS5 SQUID magnetometer with an applied field of 1 T.

$[Fe^{II}(adpt)_2(Cl)_2] \cdot 2MeOH$. A yellow solution of $FeCl_2 \cdot 4H_2O$ (83 mg, 0.42 mmol) in methanol (10 mL) was added to a colorless solution of **adpt** (200 mg, 0.84 mmol) in methanol (10 mL). The resulting orange solution was stirred at room temperature for 2 h before it was subjected to vapor diffusion of diethyl ether. This resulted in the formation of orange crystals which were identified by X-ray diffraction as the mononuclear complex $[Fe^{II}(\mathbf{adpt})_2(Cl)_2] \cdot 2MeOH$. A sample of this material gave, after drying in air (102 mg, 36% yield), an elemental analysis consistent with the composition $Fe^{II}(\mathbf{adpt})_2(Cl)_2(MeOH)_{1.5}(H_2O)_{1.5}$. Anal. Calcd for $C_{25.5}H_{29}Cl_2FeN_{12}O_3$ (678.34 g mol^{-1}): C 45.15, H 4.31, N 24.78, Cl 10.45. Found: C 45.32, H 4.01, N 24.87, Cl 10.96%. IR (KBr): 3406, 3218, 3126, 1635, 1603, 1591, 1570, 1534, 1516, 1489, 1452, 1427, 1299, 1256, 1153, 1107, 1084, 1051, 1012, 985, 794, 748, 697, 636, 606, 492, 450, 416 cm^{-1}.

$[Fe^{II}(pldpt)_2(Cl)_2] \cdot 2MeOH \cdot H_2O$. A yellow solution of $FeCl_2 \cdot 4H_2O$ (69 mg, 0.35 mmol) in methanol (10 mL) was added to a colorless solution of **pldpt** (200 mg, 0.69 mmol) in methanol (10 mL). The resulting orange solution was stirred at room temperature for 2 h before it was subjected to vapor diffusion of diethyl ether. This resulted in the formation of orange crystals which were identified by X-ray diffraction as the mononuclear complex $[Fe^{II}(\mathbf{pldpt})_2(Cl)_2] \cdot 2MeOH \cdot H_2O$. A sample of this material gave, after drying in air (186 mg, 68% yield), an elemental analysis consistent with the composition $Fe^{II}(\mathbf{pldpt})_2(Cl)_2(MeOH)_2(H_2O)$. Anal. Calcd for $C_{34}H_{34}Cl_2N_{12}O_3Fe$ (785.48 g mol^{-1}): C 51.99, H 4.36, N 21.40, Cl 9.03. Found: C 52.11, H 4.43, N 20.83, Cl 8.93%. IR (KBr): 3287, 3128, 3107, 2825, 1602, 1586, 1570, 1551, 1504, 1477, 1466, 1452, 1429, 1364, 1342, 1296, 1260, 1184, 1155, 1090, 1075, 1051, 991, 981, 913, 840, 794, 747, 727, 698, 640, 615, 572, 414 cm^{-1}.

$[Fe^{II}_2(adpt)_2(H_2O)_{1.5}(CH_3CN)_{2.5}](BF_4)_4$. A clear colorless solution of $Fe(BF_4)_2 \cdot 6H_2O$ (710 mg, 2.1 mmol) in acetonitrile (5 mL) was added dropwise to a colorless solution of **adpt** (100 mg, 0.4 mmol) in acetonitrile (10 mL). The resulting red solution was stirred at room temperature for 2 h before being subjected to vapor diffusion of diethyl ether. This resulted in the formation of yellow crystals which were identified by X-ray diffraction as the dinuclear complex $[Fe_2(\mathbf{adpt})_2(H_2O)_{1.5}(CH_3CN)_{2.5}](BF_4)_4$. A sample of this material gave, after drying in air (113 mg, 28%), an elemental analysis consistent with the composition $[Fe_2(\mathbf{adpt})_2(H_2O)_4](BF_4)_4$. Anal. Calcd for $C_{24}H_{28}B_4F_{16}Fe_2N_{12}O_4$ (1007.04 g mol^{-1}): C 28.62, H 2.80, N 16.68. Found C 28.91, H 3.01, N 16.85% IR (KBr): 3372, 1630, 1606, 1575, 1511, 1468, 1434, 1382, 1305, 1299, 1262, 1034, 1000, 801, 792, 771, 766, 753, 739, 700, 668, 635, 533, 521, 490, 469, 413 cm^{-1}.

$[Fe^{II}_2(pldpt)_2(H_2O)_2(CH_3CN)_2](BF_4)_4$. A clear colorless solution of $Fe(BF_4)_2 \cdot 6H_2O$ (88 mg, 0.26 mmol) in acetonitrile (3 mL) was

Table 2. Crystal Structure Determination Details for the Complexes $[Fe^{II}(\mathbf{adpt})_2(Cl)_2] \cdot 2MeOH$, $[Fe^{II}(\mathbf{pldpt})_2(Cl)_2] \cdot 2MeOH \cdot H_2O$, $[Fe^{II}_2(\mathbf{pldpt})_2(H_2O)_2(CH_3CN)_2](ClO_4)_4$, $[Fe^{II}_2(\mathbf{pldpt})_2(H_2O)_2(CH_3CN)_2](BF_4)_4$, and $[Fe^{II}(\mathbf{adpt})_2(py)_2](BF_4)_2 \cdot 2.4py \cdot 0.6Et_2O$

	$[Fe^{II}(\mathbf{adpt})_2(Cl)_2] \cdot 2MeOH$	$[Fe^{II}(\mathbf{pldpt})_2(Cl)_2] \cdot 2MeOH \cdot H_2O$	$[Fe^{II}_2(\mathbf{pldpt})_2(H_2O)_2(CH_3CN)_2](ClO_4)_4$	$[Fe^{II}_2(\mathbf{pldpt})_2(H_2O)_2(CH_3CN)_2](BF_4)_4$	$[Fe^{II}(\mathbf{adpt})_2(py)_2](BF_4)_2 \cdot 2.4py \cdot 0.6Et_2O$
empirical formula	$C_{26}H_{28}Cl_2FeN_{12}O_2$	$C_{32}H_{32}Cl_2FeN_{12}O_2$	$C_{36}H_{34}Cl_4Fe_2N_{14}O_{18}$	$C_{36}H_{34}B_4F_{16}Fe_2N_{16}O_2$	$C_{48.40}H_{48}B_2F_8Fe\ N_{16.40}\ O_{0.60}$
M_r	667.35	767.47	1204.27	1153.71	1098.50
crystal system	monoclinic	triclinic	triclinic	triclinic	triclinic
space group	$C2/c$	$P\bar{1}$	$P\bar{1}$	$P\bar{1}$	$P\bar{1}$
a [Å]	20.4943(11)	8.466(2)	9.9054(2)	9.9174(3)	12.406(5)
b [Å]	11.0559(5)	9.803(2)	10.59000(10)	10.4217(3)	13.561(5)
c [Å]	16.5330(8)	12.306(3)	11.9256(2)	11.8950(3)	16.564(5)
α [deg]	90	69.376(11)	76.9190(10)	76.9690(10)	73.621(5)
β [deg]	128.057(2)	75.562(13)	74.9540(10)	74.4090(10)	70.390(5)
γ [deg]	90	75.384(11)	85.4920(10)	85.335(2)	84.548(5)
V Å^3]	2949.7(3)	910.2(4)	1176.48(3)	1153.41(6)	2518.5(16)
Z	4	1	1	1	2
ρ_{calcd}.[g/cm^3]	1.503	1.400	1.700	1.661	1.449
μ [mm^{-1}]	0.741	0.611	0.934	0.746	0.385
F(000)	1376	396	612	580	1132
temperature [K]	85	85	83	87	93
crystal description	orange prism	orange prism	yellow block	yellow block	red rod
crystal size [mm]	0.12 × 0.08 × 0.04	0.24 × 0.24 × 0.10	0.32 × 0.30 × 0.26	0.70 × 0.50 × 0.50	0.21 × 0.09 × 0.08
θ range for data collection [deg]	2.23 to 26.40	2.26 to 26.67	1.81 to 25.71	2.41 to 26.42	1.35 to 26.50
reflections collected	115105	20473	4452	19894	35505
independent reflections	3031	3795	4452	4721	10259
R(int)/R(sig)	0.0358/0.0127	0.0290/0.0181	0.0181/0.0239	0.0273/0.0193	0.0418/0.0568
ratio T_{min}/T_{max}	0.847	0.921	0.699/0.615	0.755	0.907
data/restraints/parameters	3031/0/206	3795/0/237	4452/0/343	4721/0/343	10259/22/779
GOF (F^2)	1.102	1.088	1.043	1.049	1.011
$R1/wR2$ [$I > 2\sigma(I)$]	0.0358/0.0925	0.0269/0.0739	0.0287/0.0711	0.0280/0.0772	0.0448/0.1001
$R1/wR2$ (all data)	0.0390/0.0948	0.0277/0.0744	0.0329/0.0739	0.0290/0.0782	0.0793/0.1131
Max. peak/hole (e Å^{-3})	0.809/−0.736	0.318/−0.252	0.337/−0.452	0.846/−0.364	0.449/−0.537

added to a colorless solution of **pldpt** (38 mg, 0.13 mmol) in acetonitrile (3 mL). The resulting orange solution was stirred at room temperature for 2 h before it was subjected to vapor diffusion of diethyl ether. This resulted in the formation of yellow crystals which were identified by X-ray diffraction as the dinuclear complex $[Fe_2^{II}(\mathbf{pldpt})_2(H_2O)_2(CH_3CN)_2](BF_4)_4$. A sample of this material gave, after drying in air (35 mg, 23% yield), an elemental analysis consistent with the composition $Fe_2^{II}(\mathbf{pldpt})_2(H_2O)_4(CH_3CN)(BF_4)_4$. Anal. Calcd for $C_{34}H_{35}B_4F_{16}Fe_2N_{13}O_4$ (1148.65 g mol^{-1}): C 35.55, H 3.07, N 15.85. Found: C 35.67, H 3.17, N 15.75%. IR (KBr): 1605, 1540, 1514, 1471, 1438, 1351, 1299, 1263, 1061, 911, 792, 773, 695, 651, 634, 533, 521, 410 cm^{-1}.

$[Fe^{II}_2(pldpt)_2(H_2O)_2(CH_3CN)_2](ClO_4)_4$. Yellow single crystals were obtained from a 1:1 reaction in MeCN followed by vapor diffusion of Et_2O. The crystal structure determination showed this complex to be isomorphous with the BF_4 analogue. For completeness this structure has also been deposited in the Cambridge Crystallographic Data Centre (CCDC).

$[Fe^{II}(adpt)_2(py)_2](BF_4)_2$. A green solution of $Fe(BF_4)_2 \cdot 6H_2O$ (135 mg, 0.4 mmol) in pyridine (2 mL) was added to a colorless solution of **adpt** (50 mg, 0.2 mmol) in pyridine (5 mL). The resulting deep red solution was stirred at room temperature for 1 h before it was subjected to vapor diffusion of diethyl ether. This resulted in the formation of a white precipitate and dark red crystals, which were identified by X-ray crystallography to be $[Fe^{II}(\mathbf{adpt})_2(py)_2](BF_4)_4 \cdot 2.4py \cdot 0.6Et_2O$. Filtering and washing with methanol left only the red crystals which, after drying in air (18 mg, 11% yield), gave an elemental analysis consistent with the composition $[Fe^{II}(\mathbf{adpt})_2(py)](BF_4)_2$. Anal. Calcd for $C_{29}H_{25}B_2F_8FeN_{13}$ (785.06 g mol^{-1}): C 44.37, H 3.21, N 23.19. Found: C 44.36, H 3.25, N 23.29%. IR (KBr): 3295, 1635, 1608, 1589, 1568, 1534, 1487, 1450, 1427, 1291, 1254, 1054, 792, 756, 693, 637, 613, 533, 521, 467 cm^{-1}.

Crystal Structure Determinations. For the structure determination of $[Fe^{II}_2(\mathbf{pldpt})_2(H_2O)_2(CH_3CN)_2](ClO_4)_4$ the data were collected with a Bruker SMART diffractometer (University of Auckland). The data for all other structures were collected on a Bruker Kappa Apex II CCD area detector diffractometer (University of Otago). In all cases graphite-monochromated Mo Kα radiation (λ = 0.71073 Å) was used. The data were collected at low temperature as detailed in Table 2. All data sets were corrected for absorption using SADABS.[34,35] The structures were solved using SHELXS-97.[36] All structures were refined against F^2 using all data by full matrix least-squares techniques with SHELXL-97.[36] All non-hydrogen atoms were refined anisotropically. Hydrogen atoms were placed at calculated positions and refined using a riding model except for those of the H_2O, MeOH, and the amino 4-substituent which were treated as stated in the Supporting Information. All hydrogen atoms had thermal parameters 1.2 times the equivalent isotropic thermal parameters of the attached atom, except for $[Fe^{II}_2(\mathbf{pldpt})_2(H_2O)_2(CH_3CN)_2](BF_4)_4$ for which the U_{iso} values for the water hydrogen atoms were freely refined. For all compounds with partial occupancy and/or disorder, occupancies were initially freely refined then fixed. Crystal structure determination details are summarized in Table 2. CCDC 690131-690135 contains the supplementary crystallographic data for this paper and can be obtained free of charge via www.ccdc.cam.ac.uk/conts/retrieving.html.

Acknowledgment. We thank T. Groutso and Assoc. Prof. P.D.W. Boyd (University of Auckland) for the X-ray data collection on $[Fe^{II}_2(\mathbf{pldpt})_2(H_2O)_2(CH_3CN)_2](ClO_4)_4$. This work was supported by the University of Otago, including a University of Otago Research Grant (A.N. and S.B.). We thank the Tertiary Education Commission (New Zealand) for the award of a Bright Futures Top Achiever Doctoral scholarship to J.A.K., the MacDiarmid Institute for Advanced Materials and Nanotechnology (S.B.), and the Marsden Fund, RSNZ (C.B. and S.B.).

Supporting Information Available: Crystallographic data in CIF format, X-ray crystal structure refinement and SQUEEZE details, additional views of packing and VT magnetic data for $[Fe^{II}(\mathbf{adpt})_2(py)_2](BF_4)_2$. This material is available free of charge via the Internet at http://pubs.acs.org.

IC801039J

(34) Sheldrick, G. M. *SADABS. Empirical absorption correction program for area detector data*; University of Göttingen: Göttingen, Germany, 1996.
(35) Blessing, R. H. *Acta Crystallogr., Sect. A* **1995**, *51*, 33–38.
(36) Sheldrick, G. M. *Acta Crystallogr., Sect. A* **2008**, *A64*, 112–122.